Calculation of Electric Fields and Current Densities in Human Models at 50 Hz Using Finite Element method.

Dr. Farag Mahmoud Ali   ***Dr. Abd El-Naser AbuBaker Al-Beshti***

Department of Physics - Faculty of Science
Zawia University

Abstract:

The interaction of Extremely Low Frequency (ELF) electric field in human models can be described in quantitative manner through the use of Maxwell’s equations. In the present study analysis of the induced current densities in human body were carried out using axi-symmetry finite elements method. Calculations of induced electric field and current densities were carried out for two models A and B. under excitation by uniform electric field of frequency 50 Hz at 1 Kv, electric field, which was vertically described with respect to upright human models. Two configurations were considered namely, the model placed 14 mm above and in electrical contact with perfectly conducting ground. The electric field distribution and current densities in the two models A and B resulting

from the exposure to 1 Kv/m indicate pronounced differences between the two models.

1. Introduction:

It is a well-established fact that either exposure to electric or magnetic fields results in induction of electric fields and currents in biological tissues. Beginning with publication of the original [1] concern has gradually increased about the possible health impact of exposure in EMFs. Numerical methods are often employed to determine the field distributions within or around a human body from realistic electromagnetic sources. Varies articles have been published in the field of numerical computation of induced fields in a human body [2-3]. Numerical techniques used range from solution of the integral equation by the method of moments [4-5] to the finite element method [6], to the boundary element method [7] and the finite difference technique [8-9]. Computational dosimetry of contact currents for human models has been recently performed [10-11]. However, all these suggested models did not satisfy realistic conditions of human organs and geometry and then lead to discrepancy between the calculated values of the fields and those measured experimentally. This paper focus on quantifying the ELF electric field by assuming the models (low and high resolution namely A and B), Finite elements method using Galerkin approach [15] was applied to the analysis of current densities and field strengths inside a model. Mawell's equations in differential form are solved to obtain the harmonic electric field.

2. Human Body Model:

The finite element method applied on human models were modeled with low (homogeneity) and high resolution heterogeneity) namely A and B (Fig.1-2). In case of low resolution, the calculations were performed using a mesh for an overall domain composed of *553* triangles the conductivity and permittivity of the body tissue are constant at any portion of the body where the conductivity (σ) is 0.047 S/m. which corresponds to those of brain tissue [12] and permittivity (ε) is $10^6\varepsilon_0$ c, F/m. In case of high resolution the number of nodes was 752 with 1377 triangle elements. The conductivities of the various tissues at 50 Hz inside the model were assigned a recently values [13-14].

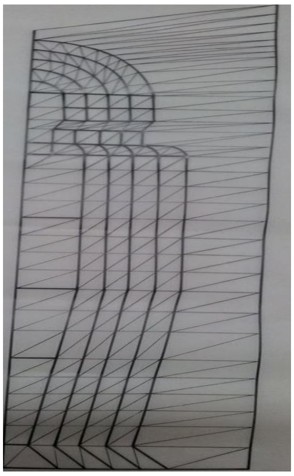

Fig. (1) Human model A

Fig. (2) Human model B

3. Numerical methods:

3.1 Assumption:

A two-dimensional domain is described in terms of Cartesian coordinates (x,y). An object representing the model of maximum dimension L and electrical conductivity (σ), permittivity (ε) respectively located as shown in this domain (Fig.1-2) and subjected to time harmonic electric field $E=E_0e^{jwt}$. The domain is assumed to be composed of two simply connected regions one of them is conducting and the other is the free space. It is assumed that the applied field frequency is sufficiently low that the body is much smaller than both the free-space wavelength

$L<<\lambda<<2\pi/\omega$, and the skin depth, $\delta = (\omega\mu s//2)^{-½}$, so that quasi-static condition is satisfied.

3.2 The finite element method:

The target body is split into triangle cells as shown in Fig. (1-2). The governing equation for the system is:

$\delta\nabla^2\phi=0$... (1)

This equation is applied for governing the voltage distribution (ϕ) in a human body. The domain is formulated as follows:

Governing equations

in human body

$\nabla^2\phi_1=0$...................................(2)

In empty

$\nabla^2\phi_2=0$...................................(3)

Boundary conditions

ϕ = prescribed value (1000 Volt)......(4)

$\frac{\partial\Phi}{\partial n}=0$ .... (5)

On the interface

$\phi_1=\phi_2$ ....(6)

$\nabla\phi_1-\nabla\phi_2=\frac{\delta}{\varepsilon_0}$ ....(7)

Finite element analysis is presented here for the governing basic equation using linear triangle elements (eq.1) with the appropriate boundary conditions of eqns.(2-7) formulated using the galerkin procedure (15) with interpolation functions as a weighted residual to derive the finite element equation.

4. Results:

4. 1 total induced current:

Calculation of induced electric field and current densities were carried out for excitation by uniform 50 Hz, 1-kV/m vertical electric field. The induced current density on the surface of the model are expressed in terms of Maxwell's displacement current ($\varepsilon\omega E_s$) where E_s is a local surface electric field. Thus, the total induced current can be calculated through the use of the following equation:

$I_s = \varepsilon_o\omega \int E_s ds$……..…………………………..….(8)

Where s is the surface area Fig. (3) shows the calculated values of total induced current on the two human models as a function of height. The data in figure are similar to those obtained by (2). The analytical expression which best fits the calculated results of the total currents induced in the human body could be written as

$I_s = 5.4.\ 10^{-9}.H^2.f/60$……..…………………….….(9)

Where H is the height of the model in m. This expression applies to the case where a man has both hands by the side of the body.

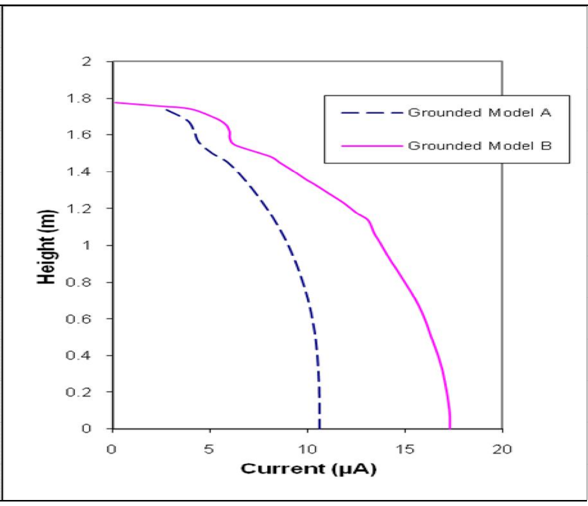

Fig.(3) : Cummulative distribution of the surface current for model A and B in 50 Hz vertical electric field of 1-kV/m: in contact with perfect ground (GD)

4.2. Internal electric field and current density

Fig. (4-5) show the calculated values of the field strengths (mV/m) distribution and current densities (mA/m^2) in the longitudinal section inside model A resulting from the exposure to an external field strengths (1-kV/m). Each figure contains two curves; the dotted curve is for 14 mm above perfect ground while the solid curve pertains to ground case.

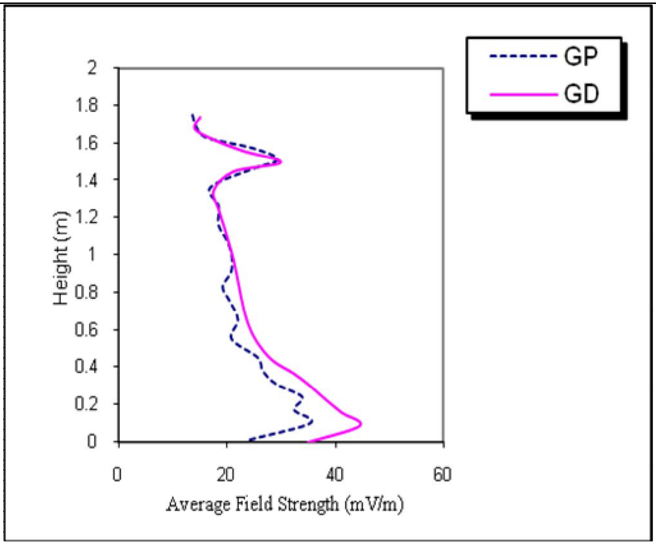

Fig.(4): Low resolution electric field distribution for model A in 50-Hz vertical electric field of 1-kV/m: 14 mm above a perfect ground (GP); and in contact with perfect ground (GD).

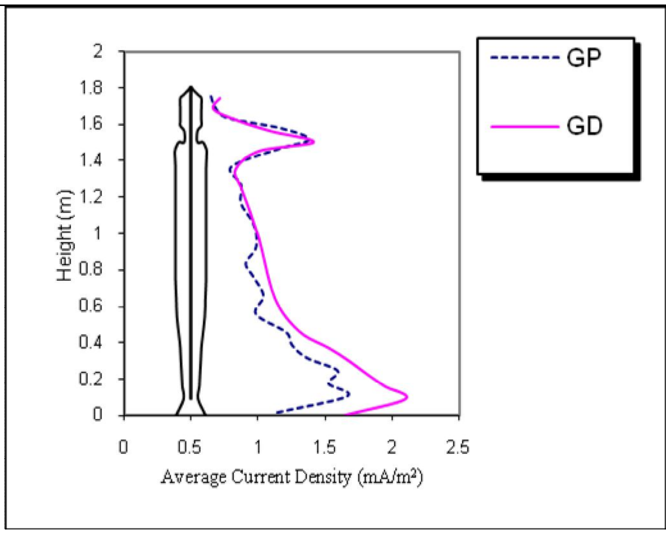

Fig.(5): Low resolution current density for model A in 50-Hz vertical electric field of 1-kV/m: 14 mm above a perfect ground (GP); and in contact with perfect ground (GD).

The results of the numerical calculations for the electric field intensity and current density distribution resulting from the exposure of the model B to 1-kV/m, 50 Hz electric field in the vertical direction are shown in Fig. *(6-7)* respectively. The dark line in the figures is for the model directly contacted with ground and the dotted line is for the insulated model from the ground.

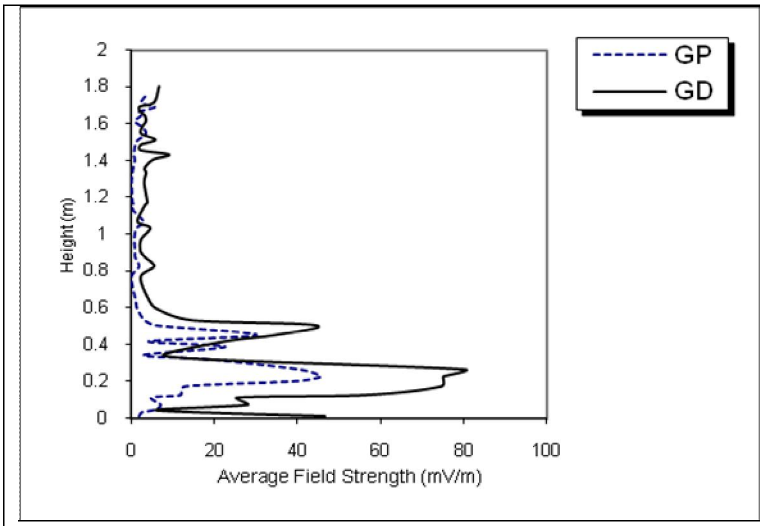

Fig.(6): High resolution electric field distribution for model B in 50-Hz vertical electric field of 1-kV/m: 14 mm above a perfect ground (GP); and in contact with perfect ground (GD).

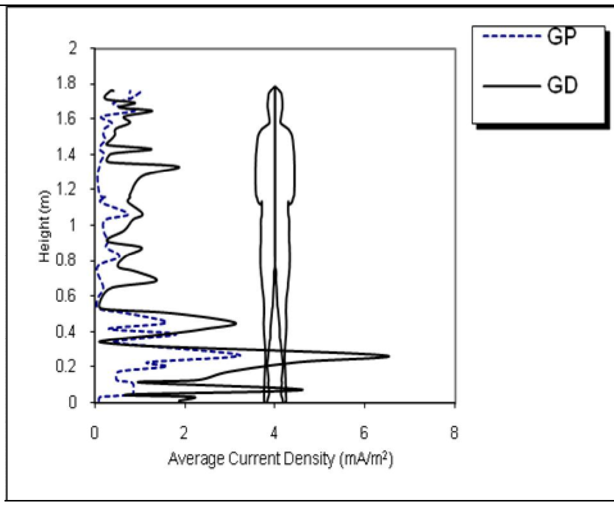

Fig.(7): High resolution current density for model B in 50-Hz vertical electric field of 1-kV/m: 14 mm above a perfect ground (GP); and in contact with perfect ground (GD).

5. Discussion:

The electric field distribution and current densities in the two models A and B resulting from the exposure to 1-kV/m as shown in (Fig. 3-7) indicate pronounced differences between the two models. However, the calculated data for model A are supported by previous findings of (6-7) and (11). In model B where the electrical conductivity of the different organs were considered, the value of the induced electric filed strengths and current densities in the different organs are much higher than for model A.

Cross section of the body parts play very important role in producing the high values in the ankle region. According to the large cross section in the neck as well as the chest regions due to the presence of arm (model A) laying in electrically contact with the body, so the upper part of the body is large and this in turn reduced the current flowing through this parts. The calculated values for these field strengths and current densities for model B are similar to those previously (3) and (9). Where their calculation depends on the application of finite difference method and use of horizontal cross section in the model, while in the present study a longitudinal cross section was applied using finite element. The present work gives more accurate results due to the capability of the finite element method to deal with complex geometry such as human body.

References:

(1) Wertheimer, N. and Leeper, E. (1979). Electrical wiring configurations and childhood cancer. Am.J.Epidemiol. 109:273-284.

(2) Gandhi, O.P. and Chen, J.Y. Numerical Dosimetry at Power line Frequencies using Anatomically Based Models. Bioelectromagnetics Suppl., 1:43-60, 1992

(3) Krajewski, W. Numerical Assessment of Electromagnetic Exposure During Live-line Works on High-voltage Objects, IET Sci. Meas. Technol., vol 3 no. 1. Pp. 27-38, 2009.

(4) Spiegel R.J. (1981). Numerical determination of induced currents in human and baboons exposed to 60 Hz electric fields. IEEE Trans. Electromagn. Compt. 23:382-390

(5) Deno, D. and Zaffanella, L. (1982). Field effects of overhead transmission lines and stations. Transmission line Reference Book: 345 kV and above 2nd Ed. (Palo Alto, CA:EPRI) pp 365-375.

(6) Chen, K. M., Chuang, H.R. and Lin, C.J. (1986). Quantification of interaction between ELF-LF electric fields and human bodies. IEEE Trans.Biomed.Eng. 33:1273-1276.

(7) Chiba, A., Isaka, K., Yokoi, Y., Nagata, M., Kitagwa, M. and Matsuo, T. (1984). Application of finite element method to analysis of induced current densities inside human model exposed to 60 Hz electric field. IEEE Trans. Power Apparatus Syst. 103:1895-1902.

(8) Peratt, A., Gonzalez, C. and Poljak, D. (2007). Current density induced in the human body due to power distributions lines using the boundary element method. J. Comm. Soft. Syst. 3(1):11-16.

(9) Dimbylow, P. (1987). Finite difference calculations of current densities in a homogeneous model of a man exposed to extremely low frequency electric fields. Bioelectromagnetics 8(4):355-375.

(10) Potter, M., okoniewski, M., and Stuchly, M.A. (2000). Low frequency finite difference time domain (FDTD) for modeling of induced fields in human close to line sources. J. Comput. Phys. 162(1):82-103.

(11) Scorretti, R. Perrussel, R., Morel, L., Burais, N., and Nicolas, L. (2010). Numerical dosimetry of currents induced in the human body by ELF magnetic fields. The International Journal for Computation and Mathematics in Electrical and Electronic Engineering 29(6):1425-1434.

(12) Chan, K.H., Hattori, J. Laakso, I. Hirata, A and Taki, M. (2013). Computational dosimetry for grounded and ungrounded human models due to contact current. Phys. Med. Biol. 58:5153

(13) Spiegel R.J. (1977). High-voltage electric field coupling to human using moment method techniques. IEEE Trans, Biomed. Eng. 24:466-472.

(14) Gabriel, S., Lan, R. and Gabriel, C. (1996). The dielectric properties of biological tissues. II. Measurements in the frequency range 10 Hz to 20 GHz. Phys. Med. Biol. 41:2251-2269.

(15) Foster, K. R. and Schwan, H.P. (1986). Dielectric properties of tissues. In CRC handbook of Biological Effects of Electromagnetic Fields, Polk, C. & Postow, E. (eds.) pp. 27-96. CRC, Press, Inc: Boca Raton, FL.

(16) Zienkiewicz, O. C. (1977). The finite element method. 3^{rd} edition, McGrew Hill.